Structural and magnetic properties of Fe_n clusters at the Al (001) surface: Early transition from paramagnetic to ferromagnetic Fe_n

R. Robles,[1] R. C. Longo,[2] E. G. Noya,[2] A. Vega,[1] and L. J. Gallego[2]
[1]*Departamento de Física Teórica, Atómica, Molecular y Nuclear, Universidad de Valladolid, E-47011 Valladolid, Spain*
[2]*Departamento de Física de la Materia Condensada, Facultad de Física, Universidad de Santiago de Compostela, E-15782 Santiago de Compostela, Spain*

(Received 22 October 2002; revised manuscript received 4 November 2003; published 24 March 2004)

Using the (re)modified embedded atom method, an extension of the embedded atom model that includes angular forces and second-nearest-neighbor interactions, we performed quenched molecular-dynamics simulations to compute the lowest-energy structures of Fe_n clusters ($n=2-20,25$) supported on or embedded in the top few layers of the Al (001) surface. Embedded clusters were always more stable than adsorbed clusters, and formed either linear chains (for $n=3$ or 5) or warped single-layer close-packed islands (for $n=4$ or $n\geqslant 6$). Determination of the spin-polarized electronic structure using a self-consistent tight-binding method showed that, due to hybridization between the Al sp and Fe d states, the embedded Fe_n clusters are nonmagnetic for $n=2-10$. However, for larger sizes they can sustain magnetic moments.

DOI: 10.1103/PhysRevB.69.115427 PACS number(s): 61.46.+w, 75.70.Cn, 36.40.Cg

I. INTRODUCTION

The structure and properties of thin or ultrathin (monolayer range) films of transition metals (TM's) on Al surfaces has been the subject of considerable attention in recent years due to their potential technological applications as metallization layers on semiconductors[1] and thin magnetic devices.[2,3] For instance, Smith and co-workers have used high-energy ion scattering/channelling (HEIS), x-ray photoelectron spectroscopy (XPS), and low-energy ion scattering (LEIS) to analyze the growth modes, interface structures, and stoichiometries of ultrathin Ni, Pd, Fe, and Ti films deposited on single-crystal Al surfaces at room temperature.[4–11] They found that, of these four metals, only Ti grows epitaxially on the Al (001) surface; the others intermix with the substrate.

To obtain insight into the structural and electronic properties of such TM-Al systems in the initial stages of their formation, small clusters of TM atoms at Al surfaces have been investigated theoretically. In particular, we recently used the embedded atom model (EAM), with the potential proposed for Ni-Al systems by Voter and Chen,[12] to compute the ground-state structures of Ni_n clusters at the Al (001) surface.[13] Our calculations showed that embedded clusters are always more stable than adsorbed clusters. Using a self-consistent spd tight-binding (TB) method[14,15] we also showed that, due to hybridization between the Al sp and Ni d states, embedded Ni_n clusters (and adsorbed or embedded Ni monolayers) are nonmagnetic. A similar sp-d hybridization effect was later also found for Ni_n clusters at the (110) and (111) surfaces of Al.[16]

In the present paper we used a similar strategy to analyze the structures and magnetic moments of clusters of the more complex, magnetic TM Fe at the Al (001) surface. To compute the ground-state structures of the Fe_n clusters ($n=2-20,25$) we used the modified embedded atom method (MEAM) (Ref. 17) as recently extended by Baskes and co-workers[18,19] to allow its application to bcc TM's such as Fe. In previous work, the MEAM has proved capable of correct description of the ''anomalous'' outward relaxation of Al at the (001) and (111) surfaces.[20]

To analyze the magnetism of the Fe_n clusters, we used a self-consistent TB method similar to that employed in Ref. 13, which is known to describe adequately the electronic structures and itinerant magnetism of a great variety of TM systems, including free clusters,[21] supported clusters,[14] and surfaces and multilayers.[22] As will be seen, our magnetic results show that the ground-state Fe_n clusters at the Al (001) surface are nonmagnetic for $n=2-10$ due to sp-d hybridization effects, in consonance with the results obtained for Ni_n clusters at the same surface.[13] However, for larger sizes the Fe_n clusters can sustain magnetic moments, in strong contrast with Ni_n.[13]

Details of the MEAM, of the computational procedure employed to obtain the ground-state structures of Fe_n clusters at the Al (001) surface, and of the method used to determine their magnetic moments are given in Sec. II. In Sec. III we present and discuss our results, and in Sec. IV we summarize our main conclusions.

II. MODEL POTENTIAL, COMPUTATIONAL PROCEDURE, AND THEORETICAL BACKGROUND

The MEAM has been discussed in detail elsewhere,[17–19] and we give here only a brief description. As in the EAM,[23] the energy E of a system is, in practice,

$$E=\sum_i \left[F_i(\rho_i)+(1/2)\sum_{j(\neq i)} S_{ij}\phi_{ij}(R_{ij}) \right], \qquad (1)$$

where ρ_i is the background electron density at the position of atom i, $F_i(\rho_i)$ is the energy required to embed atom i into this background density, $\phi_{ij}(R_{ij})$ is the pair interaction between atoms i and j, which are separated by the distance R_{ij}, and S_{ij} is a screening function that limits the range of the pair interaction, and which is also used in the calculation of ρ_i to limit the number of contributions to this quantity. Whereas in the EAM the host electron density ρ_i is approxi-

mated by a linear superposition of spherically averaged atomic electron densities,[23] in the MEAM this approximation is augmented by angle-dependent terms.[17–19]

The embedding function F_i depends on the element that atom i is an atom of, but is blind to the source of the density ρ_i. For atoms of a particular element it is given by

$$F(\rho)=AE_c(\rho/\rho^*)\ln(\rho/\rho^*), \tag{2}$$

where A is an adjustable parameter, E_c is the zero-temperature, zero-pressure sublimation energy when the element adopts a structure of a certain reference type (e.g., fcc; the reference type is usually but not necessarily the equilibrium structural type of crystals of the element), and ρ^* is a scaling constant that improves the performance of Eq. (2), and which is appropriately taken to be ρ^0_{eq}, the background electron density at 0 K and 0 Pa when the element adopts the reference structure.

The pair interaction $\phi(R_{ij})$ for atoms of a single element is calculated by applying Eq. (1) to the reference structure type for that element, viewed as a family of structures parametrized by the nearest-neighbor distance R. Defining $E^u(R)$ as the direct energy contribution of a single atom in this structure [given by the term in square brackets in Eq. (1)], this gives

$$\psi^*(R)=E^u(R)-F[\rho^0(R)], \tag{3}$$

where $\psi^*(R)=(1/2)\Sigma_{j(\neq i)}S_{ij}\phi(R_{ij})$ and $\rho^0(R)$ is the background electron density at the sites of the reference structure with first-nearest-neighbor distance R. The right-hand side here can be evaluated by using for $E^u(R)$ the ''universal'' equation of state proposed by Rose *et al.*,[24]

$$E^u(R)=-E_c(1+a^*)e^{-a^*} \tag{4}$$

with

$$a^*=3\sqrt{(B\Omega/E_c)}(R/r_e-1), \tag{5}$$

where r_e, Ω, and B are, respectively, the nearest-neighbor distance, atomic volume, and bulk modulus of the reference structure at equilibrium. If, now, S_{ij} are such that interactions are limited to first-nearest neighbors, which are totally unscreened from each other, then $\psi^*(R)=(Z_1/2)\phi(R)$ (where Z_1 is the number of first-nearest neighbors), which allows $\phi(R)$ to be calculated from Eq. (3); this was the approach taken in pre-2000 implementations of the MEAM. However, for bcc metals such as Fe, Cr, and Mo, second-nearest neighbors are only about 15% farther away than first-nearest neighbors, and must also be taken into account. In this case, with S_{ij} that limit interactions in bcc structures to first- and second-nearest neighbors but still leave first-nearest neighbors totally unscreened from each other,

$$\psi^*(R)=(Z_1/2)\phi(R)+(Z_2S/2)\phi(aR), \tag{6}$$

where Z_2 is the number of, aR the distance to, and S the screening between second-nearest neighbors, and this can be inverted to give

$$\phi(R)=(2/Z_1)\sum_0^\infty(-Z_2S/Z_1)^n\psi^*(a^nR), \tag{7}$$

allowing $\phi(R)$ to be calculated to the required precision. When the MEAM is applied to alloys rather than elements, the pair interaction between unlike atoms is obtained, without much further complication, using average single-atom energy contributions calculated by applying the universal equation of state to a suitable intermetallic compound.[17,19]

In our MEAM calculations on $Fe_n/Al(001)$ systems in this work, the parameters for the fcc metal Al were taken from Ref. 17 and had been obtained using the earlier, first-nearest-neighbor MEAM, but for Fe we used parameters reported in Ref. 18 for the second-nearest-neighbor MEAM potential of this metal. It is worth pointing out that these Fe parameters, having been obtained by fitting the potential to data for Fe, implicitly take magnetic effects into account, as is shown in particular by the fact that, unlike the first-nearest-neighbor MEAM, the version that includes second-nearest neighbors correctly reproduces the bcc ground-state structure of bulk Fe,[18] which is induced by magnetic interactions (Fe would have a close-packed structure if it followed the general trend of the periodic table).

The Al (001) surface was modeled by the top (001) layer of a 15-layer slab of atoms with the bottom four layers fixed and periodic boundary conditions in the [100] and [010] directions. Each layer comprised 450 Al atoms. The atoms in the slab were initially arranged as in bulk Al, but before addition of the Fe atoms the top 11 layers were relaxed to the minimum energy configuration using a conjugated gradient procedure.[25] As in Ref. 13, we computed the lowest-energy structures of Fe_n clusters at the Al (001) surface by considering, for each value of n, numerous starting configurations of various shapes (some supported on the surface and others embedded in the top few layers) and calculating, for each configuration, the minimum energy of the cluster+substrate system using a quenched molecular-dynamics minimization technique.[26] In some embedded starting configurations the cluster was embedded in just one layer (each cluster shape was tried in each of the top four layers), and in others it occupied various layers. In all cases the initial positions of the displaced Al atoms lay above top-layer fourfold symmetry sites located above the embedded clusters.

Before initial relaxation, the interlayer spacing of the slab in the [001] direction was $d=a/2$, where $a=4.05$ Å is the bulk lattice constant of Al.[27] Initial relaxation (without Fe atoms) increased the top and second interlayer spaces by 2.44% and 0.18%, respectively, values which are somewhat higher than the MEAM results obtained by Wan *et al.*,[20] 0.79% and 0.06%, respectively. The predicted ''anomalous'' outward relaxation of the Al (001) surface by 2.44% is consistent with the experimental figure reported by Davis *et al.*,[28] 1.8%, and with the result obtained by Bohnen and Ho[29] using first-principles calculations, 1.2%; it is not reproduced by other semiempirical potentials (see Ref. 20).

Using the cluster geometries and interatomic distances obtained as described above, the spin-polarized electronic structures of the $Fe_n/Al(001)$ systems were determined by self-consistently solving a TB Hamiltonian for the *s*, *p*, and *d*

valence electrons in a mean-field approximation.[13–15] In the usual second quantization notation, the real-space Hamiltonian H is given by

$$H=\sum_{i,\alpha,\sigma}\epsilon_{i\alpha\sigma}N_{i\alpha\sigma}+\sum_{\substack{i,\alpha,\sigma\\ i\neq j}}t_{ij}^{\alpha\beta}c_{i\alpha\sigma}^{\dagger}c_{j\beta\sigma}, \tag{8}$$

where $c_{i\alpha\sigma}^{\dagger}$ ($c_{j\beta\sigma}$) is the operator for the creation (annihilation) of an electron with spin σ and orbital state α (β) at atomic site i (j), and $N_{i\alpha\sigma}$ is the number operator. Electron delocalization within the system is described by the hopping integrals $t_{ij}^{\alpha\beta}$, which we included up to the second neighbors and assumed to be independent of spin. The heteronuclear hoppings were calculated as the average of the corresponding homonuclear hoppings. The spin-dependent diagonal terms $\epsilon_{i\alpha\sigma}N_{i\alpha\sigma}$ include electron-electron interaction through a correction of the energy levels, the $\epsilon_{i\alpha\sigma}$ being given by

$$\epsilon_{i\alpha\sigma}=\epsilon_{i\alpha}^{0}+z_{\sigma}\sum_{\beta}(J_{i,\alpha\beta}/2)\mu_{i\beta}+\Omega_{i\alpha}, \tag{9}$$

where $\epsilon_{i\alpha}^{0}$ is the bare energy of orbital α at site i (that is, excluding Coulomb interactions), $\Omega_{i\alpha}$ are adjustable site- and orbital-dependent potentials (see below) and the second term is the correction for spin polarization of the electrons at site i ($\mu_{i\beta}=\langle N_{i\beta\uparrow}\rangle-\langle N_{i\beta\downarrow}\rangle$), that is, the local magnetic moment excluding the orbital part. In this second term, the $J_{i,\alpha\beta}$ are the exchange integrals and z_{σ} is the sign function ($z_{\uparrow}=+1$; $z_{\downarrow}=-1$). As usual, we neglected the exchange integrals involving sp electrons, taking into account only the integral corresponding to the d electrons of Fe, although we note that spin polarization of the delocalized sp band is also possible as a consequence of hybridization with the d states.

As in our recent study of Co clusters embedded in Cu surfaces,[30] the parameters of the TB model [homonuclear hoppings and the exchange integral J_{dd}(Fe)] were obtained by fitting them to TB linear muffin-tin orbital (TB-LMTO) (Refs. 31,32) results for a single system, in this case an Fe monolayer embedded two layers below the Al (001) surface (a structure hereinafter denominated $L3$Fe). The TB-LMTO method is an all-electron approach based on density-functional theory (DFT); in this work it was applied using the Perdew form of the generalized gradient approximation (GGA) for exchange and correlation.[33,34] $L3$Fe was used as the ''template'' system so as to implicitly take into account both the influence of the surface and hybridization between Fe and Al atoms, Fe clusters having been found in MEAM calculations to embed themselves in the Al substrate with two layers of Al (the surface layer and an incomplete layer of displaced atoms) lying above the cluster layer (see below); the interlayer distances in $L3$Fe were determined using the same geometrical optimization procedure as for the Al + cluster systems. In fitting the TB model to the TB-LMTO data, the TB hopping parameters were obtained by the method described by Andersen *et al.*,[31,32] which was originally developed for bulk solids but is easily adapted to structures such as $L3$Fe, and the value of J_{dd}(Fe) was then varied until the TB model gave the TB-LMTO value for the magnetic moment of the embedded Fe monolayer; the optimized value of J_{dd}(Fe) was 0.81 eV. Parametrization of the TB model by fitting it to data for a single, related system is more satisfactory than fitting it to a data set comprising properties of both the bulk minority element and those of supported and embedded monolayers, the procedure employed in our earlier study of Ni clusters at the Al (001) surface.[13] Finally, the site- and orbital-dependent potentials $\Omega_{i\alpha}$ were self-consistently determined in order to obtain the TB-LMTO sp and d occupations of $L3$Fe. This ''local neutrality'' approximation, first introduced in research on surfaces and interfaces by Victora and Falicov,[35] has been used in many studies and is justified by the fact that in TM systems the local occupations are fairly insensitive to small changes in atomic environment. The validity of making the ''local neutrality'' approximation in using the potentials $\Omega_{i\alpha}$ was corroborated by the results of TB-LMTO calculations for systems consisting of an Fe monolayer embedded either one layer below the Al (001) surface or in bulk Al, the calculated charge transfers in these systems all being the same to within 0.1 electrons.

The magnetic-moment distributions of the Fe_n/Al(001) systems were determined by integrating the majority and minority local densities of states (LDOS) up to the Fermi energy. The LDOS were obtained from the diagonal elements of the Green function, which were computed using the recursion method[36] with a sufficient number of levels in the continued fraction to ensure the stability of the results. In order to correctly simulate the semi-infinite Fe_n/Al(001) systems, the number of atoms taken into account in the calculations must be large enough to avoid the neighborhood of the embedded cluster interacting with fictitious surfaces in directions other than (001). Exactly how large the acceptable minimum number is depends on the number of levels of the continued fraction; in this work we used 12 levels of the continued fraction and between 10 212 and 16 338 atoms, depending on the cluster size.

III. RESULTS AND DISCUSSION

A. Preliminaries

As indicated in Sec. II, the parameters of the self-consistent TB method used to calculate the magnetic moments of the embedded Fe_n clusters were obtained by fitting them to TB-LMTO results for an Fe monolayer embedded two layers below the Al (001) surface ($L3$Fe). Figure 1 shows the LDOS in various (001) layers of this system as calculated using the TB and TB-LMTO methods. The TB method reproduces the shape of the TB-LMTO LDOS very well, which is an indication of the quality of the TB parametrization. Both methods show strong broadening of the effective d bandwidth, which indicates hybridization between the Al sp and Fe d states. As was shown by Vega *et al.*[15] in a study of free-standing Fe_n clusters using a TB model similar to that employed here, sp-d hybridization tends to reduce spin polarization because it increases the effective d bandwidth to beyond the magnetic saturation limit. In the case of $L3$Fe the magnetic moment per atom is $0.88\mu_B$, much lower than the value of $2.41\mu_B$ obtained for bulk bcc Fe using the TB-LMTO method with the TB interatomic distances (those

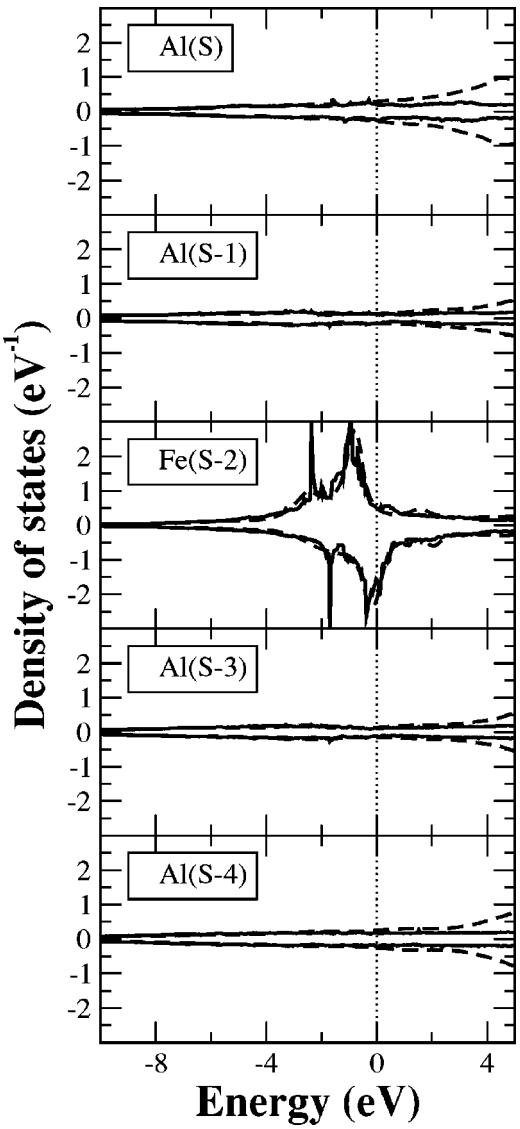

FIG. 1. LDOS in the first five layers of the system formed by an Fe monolayer embedded two layers below the Al (001) surface ($L1_2$Fe). Calculations were performed using both the TB-LMTO method (continuous line) and the TB method parametrized to reproduce these TB-LMTO results (dashed line). The vertical dotted line a 0 eV indicates the Fermi level.

obtained using the MEAM). The fact that the magnetic moment of bulk Fe given by the TB-LMTO method is slightly greater than the experimental value, $2.21\mu_B$,[27] is partly due to the use of the GGA for the exchange and correlation potential.

To test the TB parametrization, we first used it to calculate the electronic structure of an Fe monolayer supported on the Al (001) surface ($L1_1$Fe), a system which, like the Fe_n/Al(001) systems of interest, involves both surface effects and Fe-Al hybridization. The value obtained for the magnetic moment per atom, $2.12\mu_B$, agrees to within 6.6% with that afforded by TB-LMTO calculations, $2.27\mu_B$. Although broad transferability of the TB parametrization was not our purpose in this work, we also tested it on two systems that are considerably less similar than $L1_1$Fe to the fcc structure for which our parameters were optimized ($L1_2$Fe): bulk Fe, which has a bcc structure, and the ordered compound FeAl, which has a CsCl ($B2$) structure. For bulk Fe the TB and TB-LMTO results ($2.51\mu_B$ and $2.41\mu_B$, respectively) agreed to within 4%, and for FeAl they agreed to within 10% (for Fe in FeAl the TB and TB-LMTO results were $0.89\mu_B$ and $0.81\mu_B$, respectively).

We also examined the extent to which the structural predictions of the MEAM model might be flawed by the absence of explicit magnetic contributions to the energy in this model. First, we compared the TB-LMTO energy of $L1_2$Fe atoms, obtained during parametrization of the TB method, with the value obtained, likewise by TB-LMTO, when a paramagnetic solution was imposed. The difference between the two values was negligible, which is in keeping with Guenzburger and Ellis' finding that the computed energy of an $FeAl_{42}$ cluster embedded in a bulk Al potential was for all relevant Fe-Al distances virtually independent of whether calculations using DFT were performed with or without spin polarization.[37] Guenzburger and Ellis attributed this result to the fact that as the Fe-Al distance increased from the ground-state value (in which the Fe atom was nonmagnetic), the increase in $3d\uparrow$ population responsible for increasing magnetism was achieved almost exclusively at the expense of the $3d\downarrow$ population, leaving the total $3d$ population almost unchanged. In this work, our TB-LMTO results for the total $3d$ populations of magnetic and paramagnetic $L1_2$Fe were also very similar. Additional checks on the influence of magnetism on the structures of the Fe_n clusters investigated in this work are described below.

B. The main study

In the computed ground-state structures of the Fe_n/Al(001) systems investigated in this work ($n=2$-20,25), the Fe_n clusters are embedded in the second layer of the substrate, forming linear chains for $n=3$ or 5 and close-packed islands for $n=4$ and $n\geqslant 6$ (Figs. 2 and 3). That these results are very unlikely to have been influenced by the absence of explicit magnetic contributions to the energy in the MEAM was verified by using the TB method described above to calculate the electronic contributions to the energies of both magnetic and paramagnetic configurations of some of the ground-state clusters, and comparing the difference with the difference between the MEAM energies of the ground-state structure and the isomer of next lowest energy; in all cases examined, the former difference was much smaller than the latter. Since all our starting geometries assumed that the least-energy configuration of the Fe atoms would be a single cluster rather than a collection of smaller clusters or single Fe atoms, we also investigated this issue: we found that when two Fe atoms were embedded far apart from each other in the second Al layer, the total energy of the system (following relaxation) was 0.78 eV higher than when they were embedded in adjoining positions. Qualitatively, this seems likely to be due to the Al matrix being less disturbed by a cluster of Fe atoms in this layer than by a set of individual atoms. In similarly qualitative terms, the cause of the Fe atoms all lying in the second layer would seem to be

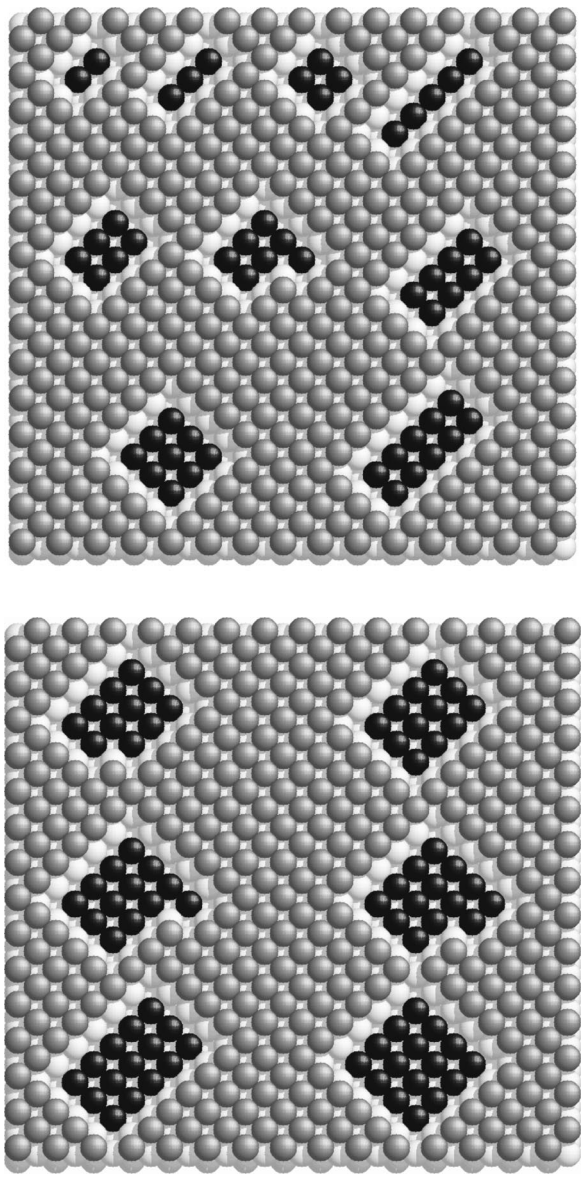

FIG. 2. Predicted ground-state structures of Fe_n clusters ($n=2-16$) at the Al (001) surface. Gray spheres represent top-layer Al atoms, white spheres second-layer Al atoms, and black spheres Fe atoms, all of which are located in the second layer. For clarity, some Al atoms of the first layer of the substrate, and the second-layer Al atoms pushed out on top of the top layer by the embedded Fe_n clusters, have been removed to allow visualization of the latter.

the relative looseness of the top Al layer (see Sec. II, paragraph 6); the Fe atoms stop burrowing as soon as they reach the more tightly packed region of the Al slab.

The structures shown in Figs. 2 and 3 are mostly similar to the ground-state structures of Ni_n clusters at the Al (001) surface, which according to our earlier calculations using the Voter and Chen[12] version of the EAM are all close-packed islands that for $n>2$ are likewise embedded in the second Al layer.[13] These results for Fe are in keeping with the general tendency of Fe atoms to embed in the Al (001) surface that was observed experimentally by Smith and co-workers,[8] and are consistent with the fact that Al has a lower surface energy

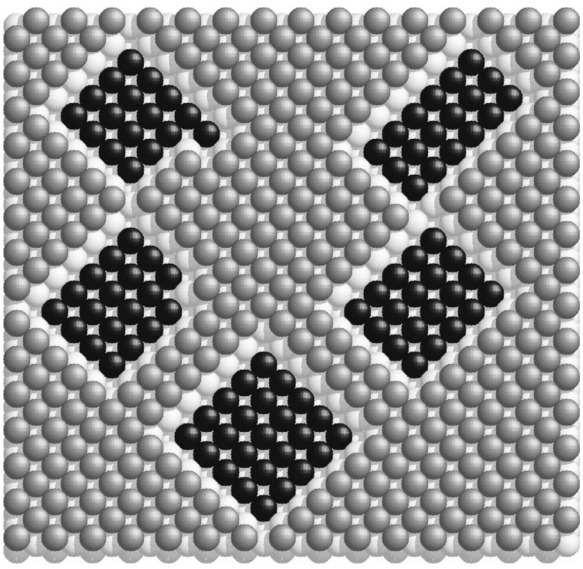

FIG. 3. As for Fig. 2, but for $n=17-20$, 25.

than Fe.[38] Although experimental results on the geometries of Fe_n clusters at the Al (001) surface are as far as we know not available for comparison, the displacements of Al atoms in the vicinity of the Fe_n clusters that are predicted by our MEAM calculations are consistent with the displacements of Al atoms measured by ion scattering experiments.[39]

The computed Fe_n structures that are illustrated in Figs. 2 and 3 are not flat but significantly warped, as Fig. 4 shows in the case of Fe_{16}. As will be seen below, this bending, which has also been found by Stepanyuk *et al.*[40] in a study of Co_n clusters *supported* on the Cu (001) surface, is crucial for explaining certain peculiarities of the magnetic behavior of the Fe_n/Al(001) systems.

In the upper panel of Fig. 5 we show the average magnetic moment per atom of the embedded Fe_n clusters as a function of n. For $n\leqslant 13$ the clusters are nonmagnetic except Fe_{11}, but for $n>13$ their average magnetic moments per atom increase monotonically with n (bar a slight oscillation around $n=18$), although that of Fe_{25} is still much lower than that of $L3$Fe, $0.88\mu_B$, which must be the value converged to as n increases.

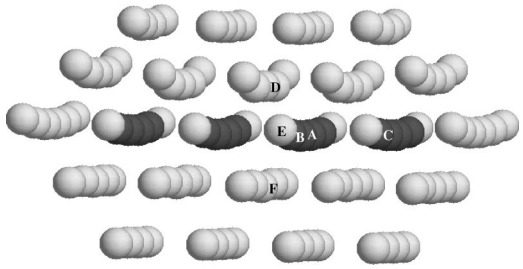

FIG. 4. Lateral view of the predicted ground-state structure of Fe_{16} at the Al (001) surface, together with part of the Al substrate. Note the warped geometry. Gray spheres represent Fe atoms, and white spheres Al atoms. The white spheres at the top of the figure represent the Al atoms pushed out on top of the top layer of the substrate by the embedded Fe_{16} cluster. Letters on some Fe and Al atoms are used to refer to these atoms in Fig. 6.

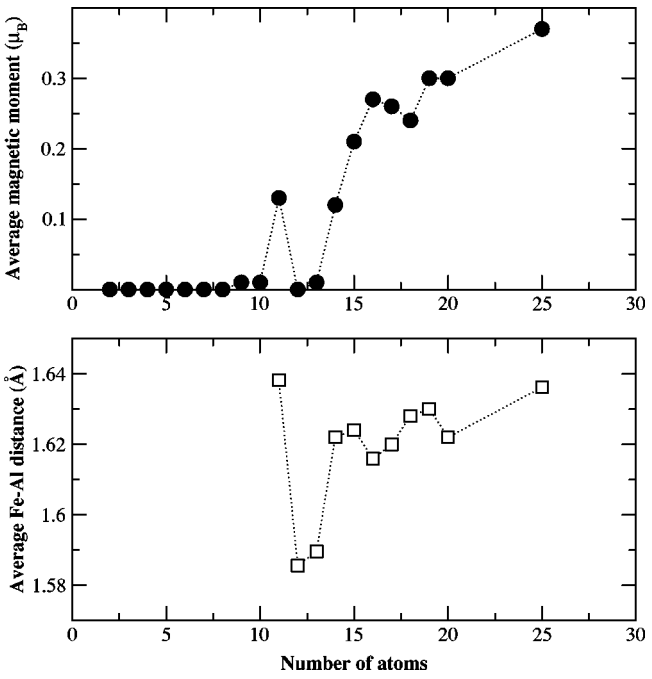

FIG. 5. Average magnetic moment per atom (in μ_B) of embedded Fe_n clusters ($n=2-20,25$), as a function of n (upper panel); and average distance (in Å) between the central atoms in these clusters ($n=11-20,25$) and the nearest Al atoms in the adjacent surface layer (lower panel).

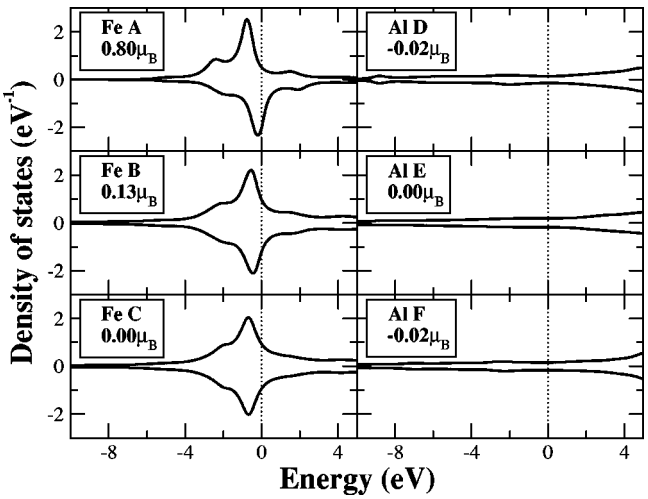

FIG. 6. LDOS at some representative inequivalent sites of the Fe_{16}/Al(001) system (those indicated by letters in Fig. 4), as calculated using the self-consistent TB model. The insets show the magnetic moments at these sites. Note the antiferromagnetic coupling between the Fe and the surrounding Al atoms. The vertical dotted lines at 0 eV indicate the Fermi level.

Detailed inspection of the magnetic-moments distribution within the magnetic Fe_n clusters reveals strong dependence on the local environment. The Fe atoms located at the center of the cluster display magnetic moments close to the magnetic moment per atom of $L1_0$Fe, $0.88\mu_B$; that of the central atom of Fe_{15}, for example, is $0.78\mu_B$. However, the outer Fe atoms have much lower moments as a consequence of greater Fe-Al hybridization and consequently decreased spin-polarization; this is illustrated in Fig. 6, which shows the magnetic moments distribution of the Fe_{16}/Al(001) system pictured in Fig. 4. The nonmagnetic electronic configuration obtained for the smaller clusters is also a consequence of Fe-Al hybridization; it is necessary to reach a critical size in order to overcome this hybridization and stabilize a magnetic moment.

The above results are consistent with the fact that starting from pure bulk Fe, the gradual replacement of Fe by Al leads to a progressive decrease of the saturation magnetization until the alloy eventually becomes nonmagnetic.[41] They are also consistent with experiments[42] and theoretical calculations[42–44] suggesting that the presence of Fe clusters in the disordered Fe-Al alloys obtained by rapid quenching or cold working may be responsible for the magnetic order that is observed even at Al concentrations of about 50% (Ref. 45), and which contrasts with the fact that the intermetallic compound FeAl is nonmagnetic.

Another general trend observed in our results is that the slight magnetic moments induced by Fe in the surrounding Al atoms are coupled antiferromagnetically with that of Fe (see, e.g., Figs. 4 and 6). This antiferromagnetic coupling at the interface is consistent with recent DFT results for free-standing Fe_nAl_m clusters ($n+m=15$) obtained by Reddy *et al.*[46], and with the experiments and theoretical results of Arrott and Sato on Fe-Al alloys.[47,48]

Finally, the irregularities in the cluster-size dependence of the average magnetic moment per atom (Fig. 5, upper panel) are attributable to the intensity of Fe-Al hybridization being influenced by the warping of the cluster and the Al layer above it (Fig. 4). In particular, inspection of Fe-Al distances shows that in Fe_{12} and Fe_{13} this warping is such that the central Fe atoms of the cluster are closer to their nearest Al atoms than in any other cluster larger than Fe_{10} (Fig. 5, lower panel), which enhances hybridization and thereby eliminates both the magnetic moment of these central atoms and, consequently, their induction of magnetic moments in the peripheral atoms. The difference in warping with respect to Fe_{11} is attributable to the replacement of the Al atom at the corner of Fe_{11} with an Fe atom (see Fig. 2): since Fe has the smaller atomic volume, this allows greater relaxation at the center of Fe_{12} and Fe_{13}, and among the overlying Al atoms, than at the center of Fe_{11}.

IV. SUMMARY AND CONCLUSIONS

In this paper we used the MEAM (Refs. 17–19) to compute the ground-state structures of Fe_n clusters ($n=2-20,25$) at the Al (001) surface, and a self-consistent TB model similar to that employed in Ref. 13 to determine their magnetic moments. We found that the Fe_n clusters are always embedded in the second layer of the substrate, forming linear chains for $n=3$ and 5 and warped close-packed islands for $n=4$ and $n\geqslant 6$. This finding, which is consistent with the tendency for Fe atoms to embed in the Al (001) substrate that was observed experimentally by Smith and co-workers,[8] is similar to that obtained for the related system Ni_n/Al (001) using the Voter and Chen version of the EAM.[13]

We also found, likewise in consonance with the results obtained for Ni_n clusters at the Al (001) surface, that the embedded Fe_n clusters are nonmagnetic for $n=2-10$, 12, and 13 due to *sp-d* hybridization effects. However, for $n=11$ and $n>13$, Fe_n clusters, unlike those of the less magnetic TM Ni, can sustain magnetic moments. The irregularity in the size dependence of average magnetic moment per atom between $n=10$ and $n=13$ is due to the distances of the central cluster atoms from their nearest Al neighbors being least for Fe_{12} and Fe_{13}, which increases the Fe-Al hybridization of these atoms. For $n>13$, the Fe_n clusters are increasingly magnetic except for a small oscillation in this trend around Fe_{18}.

Given the semiempirical character of the MEAM and TB methods used in this paper, it is probable that our structural and magnetic results differ somewhat from those that might be obtained using theoretically more accurate *ab initio* methods. In particular, our methods do not fully take into account the effects of electronic correlations on the magnetic behavior of Fe-Al systems[49,50] (no models are available that allow this for complex low-dimensional systems such as those studied here), and as other one-particle treatments (including standard DFT approaches) must therefore afford magnetic moments that are slightly too high, with the result that the paramagnetic-ferromagnetic transition may occur at a cluster size somewhat larger than that observed in this study. However, since the MEAM and TB methods are, respectively, capable of describing the structural[17–19] and electronic[14,21,22] properties of a wide range of systems, and in view of the results of the tests and checks discussed above, we believe that our results must certainly reflect the general trends of the behavior of Fe_n/Al(001) systems. In particular, the finding that a magnetic transition must occur at very small cluster sizes is of importance for both theoretical and technological reasons.

ACKNOWLEDGMENTS

We are grateful to J. García-Rodeja for helpful discussions, to M. I. Baskes for making the codes of the original MEAM available to us, and to R. J. Smith for useful information related to the experiments reported in Ref. 8. This work was supported by the Spanish Ministry of Science and Technology (MCyT) in conjunction with the European Regional Development Fund (Project Nos. MAT2002-03142 and MAT2002-04393), the Xunta de Galicia (Project No. PGIDT01PXI20605PR), and the Junta de Castilla y León (Grant No. VA 073/02). E.G.N. thanks the MCyT for an FPI grant.

[1] T. Sands, Appl. Phys. Lett. **52**, 197 (1988).
[2] T. Hamaguchi, H. Aida, S. Nakagawa, and M. Naoe, J. Appl. Phys. **73**, 6444 (1993).
[3] T. Haeiwa, H. Negoro, and M. Matsumoto, J. Appl. Phys. **69**, 5346 (1991).
[4] V. Shutthanandan, A.A. Saleh, and R.J. Smith, J. Vac. Sci. Technol. A **11**, 1780 (1993).
[5] V. Shutthanandan, A.A. Saleh, A.W. Denier van der Gon, and R.J. Smith, Phys. Rev. B **48**, 18 292 (1993).
[6] A.A. Saleh, V. Shutthanandan, and R.J. Smith, Phys. Rev. B **49**, 4908 (1994).
[7] V. Shutthanandan, A.A. Saleh, N.R. Shivaparan, and R.J. Smith, Surf. Sci. **350**, 11 (1996).
[8] N.R. Shivaparan, V. Krasemann, V. Shutthanandan, and R.J. Smith, Surf. Sci. **365**, 78 (1996).
[9] N.R. Shivaparan, V. Shutthanandan, V. Krasemann, and R.J. Smith, Surf. Sci. **373**, 221 (1997).
[10] A.A. Saleh, V. Shutthanandan, N.R. Shivaparan, R.J. Smith, T.T. Tran, and S.A. Chambers, Phys. Rev. B **56**, 9841 (1997).
[11] V. Shutthanandan, A.A. Saleh, and R.J. Smith, Surf. Sci. **450**, 204 (2000).
[12] A.F. Voter and S.P. Chen, in *Characterization of Defects in Materials*, edited by R. W. Siegel, J. R. Weertman, and R. Sinclair, Mater. Res. Soc. Symp. Proc. 82 (Materials Research Society, Pittsburgh, 1987), p. 175.
[13] R. Robles, R.C. Longo, A. Vega, and L.J. Gallego, Phys. Rev. B **62**, 11 104 (2000).
[14] J. Izquierdo, A. Vega, and L.C. Balbás, Phys. Rev. B **55**, 445 (1997).
[15] A. Vega, J. Dorantes-Dávila, L.C. Balbás, and G.M. Pastor, Phys. Rev. B **47**, 4742 (1993).
[16] R. Robles, R.C. Longo, A. Vega, C. Rey, and L.J. Gallego, Surf. Sci. **482-485**, 976 (2001).
[17] M.I. Baskes, Phys. Rev. B **46**, 2727 (1992).
[18] B.-J. Lee and M.I. Baskes, Phys. Rev. B **62**, 8564 (2000).
[19] B.-J. Lee, M.I. Baskes, H. Kim, and Y.K. Cho, Phys. Rev. B **64**, 184102 (2001).
[20] J. Wan, Y.L. Fan, D.W. Gong, S.G. Chen, and X.Q. Fan, Modell. Simul. Mater. Sci. Eng. **7**, 189 (1999).
[21] S. Bouarab, A. Vega, M.J. López, M.P. Iñiguez, and J.A. Alonso, Phys. Rev. B **55**, 13 279 (1997).
[22] A. Vega, L.C. Balbás, H. Nait-Laziz, C. Demangeat, and H. Dreyssé, Phys. Rev. B **48**, 985 (1993).
[23] S.M. Foiles, M.I. Baskes, and M.S. Daw, Phys. Rev. B **33**, 7983 (1986).
[24] J.H. Rose, J.R. Smith, F. Guinea, and J. Ferrante, Phys. Rev. B **29**, 2963 (1984).
[25] W.H. Press, B.P. Flannery, S.A. Teukolsky, and W.T. Vetterling, *Numerical Recipes* (Cambridge University Press, Cambridge, 1988).
[26] G.J. Ackland and R. Thetford, Philos. Mag. A **56**, 15 (1987).
[27] *Smithells Metals Reference Book*, edited by E.A. Brandes and G.B. Brook (Butterworth-Heinemann, Oxford, 1992).
[28] H.L. Davis, J.B. Hannon, K.B. Ray, and E.W. Plummer, Phys. Rev. Lett. **68**, 2632 (1992).
[29] K.-P. Bohnen and K.-M. Ho, Surf. Sci. **207**, 105 (1988).
[30] R. Robles, R.C. Longo, A. Vega, C. Rey, V. Stepanyuk, and L.J. Gallego, Phys. Rev. B **66**, 064410 (2002).
[31] O.K. Andersen and O. Jepsen, Phys. Rev. Lett. **53**, 2571 (1984).

[32] O.K. Andersen, O. Jepsen, and D. Glötzel, in *Hightlights of Condensed Matter Theory*, edited by F. Bassani, F. Fumi, and M. P. Tossi (North-Holland, Amsterdam, 1985), p. 59.
[33] J.P. Perdew, *Electronic Structure of Solids '91* (Akademie-Verlag, Berlin, 1991).
[34] J.P. Perdew, J.A. Chevary, S.H. Vosko, K.A. Jackson, M.R. Pederson, D.J. Singh, and C. Fiolhais, Phys. Rev. B **46**, 6671 (1992).
[35] R.H. Victora and L.M. Falicov, Phys. Rev. B **31**, 7335 (1985).
[36] R. Haydock, in *Solid State Physics*, edited by H. Ehrenreich, F. Seitz, and D. Turnbull (Academic, New York, 1980), Vol. 35, p. 215.
[37] D. Guenzburger and D.E. Ellis, Phys. Rev. Lett. **67**, 3832 (1991).
[38] J.A. Alonso and N.H. March, *Electrons in Metals and Alloys* (Academic, New York, 1989).
[39] R.J. Smith (private communication).
[40] V.S. Stepanyuk, D.V. Tsivline, D.I. Bazhanov, W. Hergert, and A.A. Katsnelson, Phys. Rev. B **63**, 235406 (2001).
[41] *Physical Properties and Other Data*, edited by H.P.J. Wijn, Landolt-Börnstein, New Series, Group III, Vol. 19, Pt. b (Springer, Berlin, 1987), pp. 295–356.
[42] J. Bogner, W. Steiner, M. Reissner, P. Mohn, P. Blaha, K. Schwarz, R. Krachler, H. Ipser, and B. Sepiol, Phys. Rev. B **58**, 14 922 (1998).
[43] N.I. Kulikov, A.V. Postnikov, G. Borstel, and J. Braun, Phys. Rev. B **59**, 6824 (1999).
[44] B.V. Reddy, S.C. Deevi, F.A. Reuse, and S.N. Khanna, Phys. Rev. B **64**, 132408 (2001).
[45] G.R. Caskey, J.M. Franz, and D.J. Sellmyer, J. Phys. Chem. Solids **34**, 1179 (1973).
[46] B.V. Reddy, S.C. Deevi, A.C. Lilly, and P. Jena, J. Phys.: Condens. Matter **13**, 8363 (2001).
[47] A. Arrott and H. Sato, Phys. Rev. **114**, 1420 (1959).
[48] H. Sato and A. Arrott, Phys. Rev. **114**, 1427 (1959).
[49] P. Mohn, C. Persson, P. Blaha, K. Schwarz, P. Novák, and H. Eschrig, Phys. Rev. Lett. **87**, 196401 (2001).
[50] D.A. Papaconstantopoulos and C.S. Hellberg, Phys. Rev. Lett. **89**, 029701 (2002).